Yin, H., Shen, X., Huang, Y., Feng, Z.，Long，Z., Duan, R., Lin, C.-H., Wei, D., Sasanapuri, B., and Chen, Q. 2016. "Modeling dynamic responses of aircraft environmental control systems by coupling with cabin thermal environment simulations," *Building Simulation*, 9(4): 459-468.

Modeling Dynamic Responses of Aircraft Environmental Control Systems by Coupling with Cabin Thermal Environment Simulations

Haishen Yin[1], Xiong Shen[1], Yan Huang[1], Ran Duan[1], Chao-Hsin Lin [2], Daniel Wei[3], Balasubramanyam Sasanapuri[4] and Qingyan Chen[1,5]

[1]Tianjin Key Laboratory of Indoor Air Environmental Quality Control, School of Environmental Science and Engineering, Tianjin University, Tianjin 300072, China
[2]Environmental Control Systems, Boeing Commercial Airplanes, Everett, WA 98203, USA
[3]Boeing Research & Technology - China, Beijing 100027, China
[4]ANSYS India Pvt Ltd, Pune, India
[5]School of Mechanical Engineering, Purdue University, West Lafayette, IN 47907, USA

Abstract

Commercial aircraft use environmental control systems (ECSs) to control the thermal environment in cabins and thus ensure passengers' safety, health, and comfort. This study investigated the interaction between ECS operation and cabin thermal environment. Simplified models were developed for the thermodynamic processes of the key ECS components in a commercial software program, ANSYS Simplorer. A computational fluid dynamics (CFD) program, ANSYS Fluent, was employed to simulate the thermal environment in a cabin. Through the coupling of Simplorer and Fluent, a PID control method was applied to the aircraft ECS in Simplorer to achieve dynamic control of the temperature of the supply air to the cabin, which was used as a Fluent input. The calculated supply air temperature agreed with the corresponding experimental data obtained from an MD-82 aircraft on the ground. The coupled model was then used to simulate a complete flight for the purpose of studying the interaction between ECS operation and the cabin thermal environment. The results show that the PID controller in the ECS can maintain the cabin air temperature within ±0.6 K of the set point, with an acceptable air temperature distribution. The coupled models can be used for the design and analysis of the ECS and cabin thermal environment for commercial airplanes.

Keywords: Thermal control, Temperature field, Aircraft ECS, Coupled Simulation

1 Introduction

Between 2005 and 2014, there were 12.6 billion air travellers worldwide, and the number is increasing (World Bank Group 2015). In order to ensure passengers' safety, health, and comfort, the thermal environment in aircraft cabins should be controlled. On the ground, an aircraft cabin can be very cold on a winter morning or very hot on a summer afternoon. It is essential that the environmental control systems (ECSs) in aircraft be

capable of quickly heating up or cooling down cabins in order to provide an acceptable thermal environment for passengers and crew members. Furthermore, during takeoff or landing the aircraft is exposed to very rapid changes in outside air temperature and pressure. For example, the outside air temperature at cruising altitude can be as low as -65 ^{o}C and the atmospheric pressure as low as 0.2 atm, while the corresponding temperature and pressure at the sea level can be close to 0 ^{o}C and 1 atm. The ground air temperature can be higher or lower than 0 ^{o}C in a typical winter day depending on the location so does the outside air temperature at the cruising height. The ECS should be able to rapidly respond to the outside environment and maintain a suitable temperature of around 20 ^{o}C and a pressure equivalent to 2440 m above sea level (0.74 atm) inside the air cabin (ASHRAE 2013).

In recent decades, there have been many investigations on ECSs and cabin environments in aircraft. Eichler (1975) established several simplified models to represent the dynamics of thermal controllers, valves, sensors, heat exchangers and turbines of the ECS. Leo and Pérez-Grande (2005) employed other simplified models to represent different ECS components in order to analyze the total performances. Zhao et al. (2009) applied an experimental method to study ECS design and recommended that off-design performance and dynamic response be taken into account in the design process. Although these studies provided meaningful results, they addressed ECS performance rather than the influence of cabin thermal environment on ECS response. However, the cabin thermal environment is important for the thermal comfort and well-being of passengers and crew. Aircraft manufacturers have tried to make a better cabin thermal environment.

Meanwhile, other studies have focused only on the cabin thermal environment. Some of them have used experimental measurements in actual airplane cabins (Liu et al. 2012a; Huang et al. 2015), mock-ups (Zhang et al. 2009), or scaled models (Poussou et al. 2010). However, the studies were intended mainly for obtaining high-quality data in order to validate numerical simulations (Liu et al. 2012b). Although these experimental measurements provided realistic information about the cabin thermal environment, they were expensive and time consuming (Liu et al. 2012b). Numerical simulations, especially the accurate and informative computational fluid dynamics (CFD) simulations, have been very popular in studying (Duan et al. 2015; Mazumdar et al. 2014; Li et al. 2015), designing (Liu and Chen 2015; Chen et al. 2014), and optimizing (Hu and You 2015) the cabin thermal environment. These studies were mainly conducted in steady state such as on ground or in cruising stage of the flight. Even though the experimental and numerical studies on cabin environment have been intensive, they have primarily addressed steady-state problems without considering the effect of the dynamic response of the ECS. The ECS should be able to response to the dynamic changes of the outside conditions so that it can provide the same comfort level from taking off to landing.

A limited number of investigations have studied the ECS and cabin air environment together. For example, Ordonez and Bejan (2003) proposed a model that coupled an ECS with a cabin with well-mixed air for analyzing the minimum power requirement for the ECS. Their results showed that ECS output was related to the inlet air conditions. Hofman (2003) combined a two-dimensional cabin model with a controller algorithm to analyze the stability and accuracy of a coupled ECS and cabin model. They found that the time step was an important factor in the model's accuracy. However, the assumption of

well-mixed cabin air and a two-dimensional cabin cannot accurately depict actual cabins with strong three-dimensional spatial variations in air distribution. Several previous studies by experimental measurements and numerical simulations (Duan et al. 2015; Mazumdar et al. 2014; Li et al. 2015, Liu et al. 2012 a,b; Huang et al. 2015) have shown that the air distributions in a cabin are highly non-uniform and three dimensional. The well-mixed or two-dimensional assumptions would not be acceptable. Even with a high air exchange rate, the air temperature stratification in the cabin can be very high before the first service in a winter morning, which may not meet the thermal comfort standard for serving passengers. In addition, the dynamic change in outside air and thermal boundary conditions and their effects on the cabin air environment should not be overlooked. Therefore, it is necessary to couple an ECS with a three-dimensional cabin environment in order to correctly simulate the dynamic response of the ECS and the thermal response of the cabin environment. The coupled simulations can provide detailed information of the three-dimensional air distribution as well as the thermodynamic performance of the ECS in responding to the dynamic changes of the outdoor conditions.

This paper reports our effort in developing a model that incorporates the interaction between an ECS and the thermal environment in an aircraft cabin. By use of the model, this investigation performed coupled, transient simulations of an ECS and a cabin environment. This investigation also conducted experimental measurements of an ECS and dynamic responses in a cabin in order to validate the numerical results.

2 Methods

To develop a model that incorporates the interaction between an ECS and the cabin thermal environment, this study first implemented simplified models for individual components of the ECS in ANSYS Simplorer, a system modeling software provided by ANSYS Corp. (ANSYS, 2014a). This investigation then used ANSYS Fluent (ANSYS, 2014b), a CFD program, to simulate air velocity and temperature distributions in an aircraft cabin. When the inputs and outputs of ANSYS Simplorer and ANSYS Fluent were coupled, these programs were able to provide each other with suitable boundary conditions. This section describes the individual models as well as the experimental facility used to obtain experimental data for model validation.

2.1 Simplified models for ECSs on the ground

When a commercial airplane is parked on the ground, a ground air-conditioning cart (GAC) or jet-bridge air-conditioning pack is used to provide air that is suitable for regulating the thermal environment in the cabin. Fig. 1 is a schematic diagram of a typical aircraft ECS as used in this study. The outside air (a) flows through the air filter and is then heated up by the heater in winter or cooled down by the cooling coil in summer, as determined by the temperature controller. Next, the heated or cooled air (b) travels to the air mixing manifold. The air from the manifold outlet (c) passes through the air supply pipelines (d) to the cabin for controlling the thermal environment. Fig. 2 is a psychrometric chart of the handling processes for the supply air in the ECS on the ground, including the GAC. The labels used for the various stages are the same in Figs. 1 and 2.

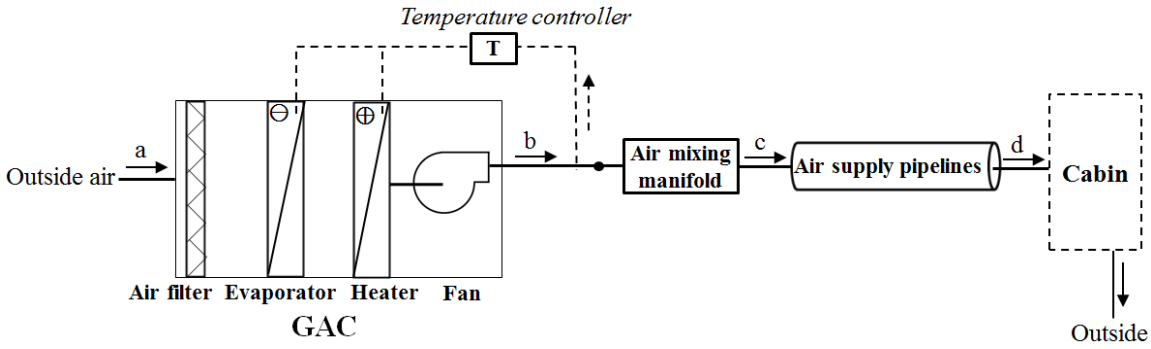

Fig. 1. Schematic of a typical aircraft ECS used on the ground with a GAC.

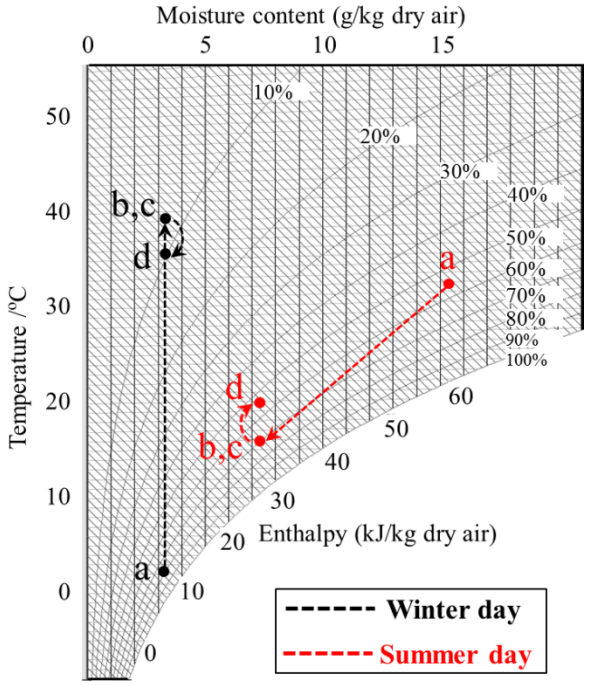

Fig. 2. Psychrometric chart of the air handling processes in the GAC and ECS on the ground.

The mass flow rate of the supply air can be controlled by the GAC according to aircraft type. The supply air temperature in the ECS on the ground can be determined by:

$$T_b^k = T_a^k + Q^k / m \ / c_p \tag{1}$$

$$T_c^k = T_b^k + Q_{bc}^k / m / c_p \tag{2}$$

$$T_d^k = T_c^k + Q_{cd}^k / m \ / c_p \tag{3}$$

where k represents different time steps; T_a^k, T_b^k, T_c^k, and T_d^k the air temperature in different components of the GAC and ECS as shown in Fig. 1; Q^k the heating load (positive value) or cooling load (negative value) of the GAC; Q_{bc}^k and Q_{cd}^k the heat gain/loss in the air mixing manifold and air supply pipelines, respectively; m the mass flow rate of the supply air; and c_p the constant-pressure specific heat capacity of air (c_p = 1.005 kJ/(kg·K)).

On the ground, the aircraft ECS controls the thermal environment in the cabin by

regulating the supply air temperature. The set-point temperature should meet the requirement of rapid heating on a winter morning or rapid cooling on a summer afternoon. The air temperature sensor is typically installed at the outlet of the GAC, as shown in Fig. 1. The temperature measured by the sensor is compared with the set-point value, and the difference is used to regulate the supply air temperature through the temperature controller by means of a PID logic controller.

2.2 Simplified models of ECSs in flight

Most aircraft ECSs use a typical Brayton cycle to handle the air in flight (Pérez-Grande and Leo 2002). Fig. 3 is a schematic of the typical ECS that was used in the current study. The key components of this simple ECS include heat exchangers, a compressor, a turbine, a flow valve, pipelines, etc., which together can perform the essential functions of an environmental control system. The bleed air (1) is compressed air from the aircraft engine that is at high temperature and pressure before entering the ECS. Most of the bleed air (2) travels to the primary heat exchanger and is precooled (3) by the ram air (r2) from outside. The compressor further pressurizes the air (3) and also increases its temperature (4). The hot air (4) is then cooled down (5) in the main heat exchanger by the ram air (r1). A turbine cools the air further in order to provide cooling capability, while the air pressure also becomes lower at the turbine exit (6). The cool air (6) is then mixed with part of the bleed air (11) to a suitable temperature (7) for mixing with the recycled air (10) in the air mixing manifold. The air from the manifold (8) is finally delivered to the air cabin (9) through supply pipelines. Fig. 4 is a T-s chart of the handling processes for the supply air in the ECS in the cruising state. The labels used for the various stages in Figs. 3 and 4 are the same.

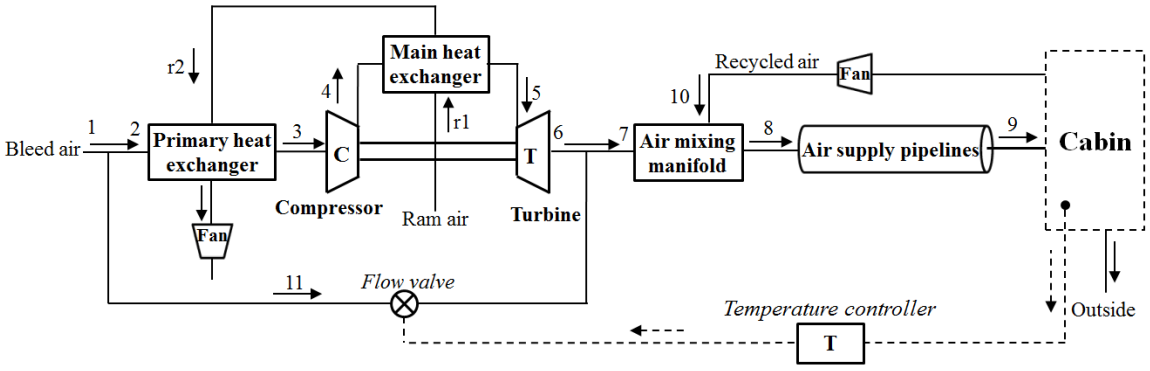

Fig. 3. Schematic of the typical aircraft ECS used in flight in this study.

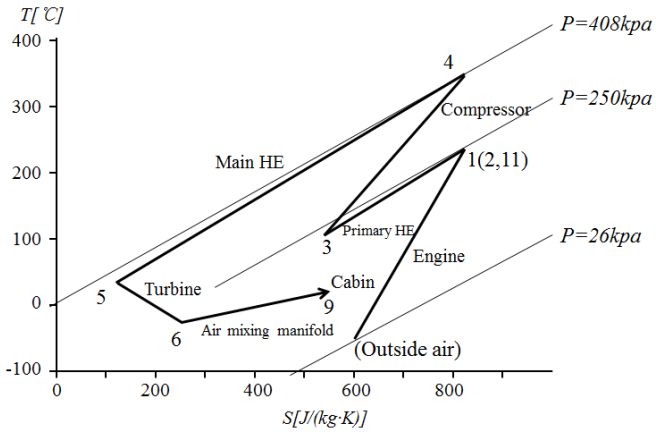

Fig. 4. A T-s diagram of the air handling processes in ECS components in the cruising state.

The mass flow rate and air temperature for each of the handling processes in the ECS were calculated by use of the models developed by Pérez-Grande and Leo (2002) and summarized in Table 1.

Table 1. Simplified models for the ECS components in flight.

ECS components or pipes	Mass flow rate (kg/s)	Temperature (K)
ECS inlet	$Q_1=Nq$	$T_1=473$ *(Constant)*
Bleed air pipe	$Q_2=Q_1-Q_{11}$	$T_2=T_1$
Primary heat exchanger	$Q_3=Q_2$	$T_3=(1-\eta_{PHE})T_2+\eta_{PHE}T_{r2}$
Compressor	$Q_4=Q_3$	$T_4=T_3[1+(\pi_c^{1-1/k}-1)/\eta_c]$
Main heat exchanger	$Q_5=Q_4$	$T_5=(1-\eta_{MHE})T_4+\eta_{mHE}T_{r1}$
Turbine	$Q_6=Q_5$	$T_6=T_5[1-\eta_t(1-\pi^{1/k-1})]$
Air mixing manifold inlet	$Q_7=Q_1=Q_6+Q_{11}$	$T_7=(Q_6T_6+Q_{11}T_{11})/Q_7$
Air mixing manifold outlet	$Q_8=Q_7+Q_{10}$	$T_8=(Q_7T_7+Q_{10}T_{10})/(Q_7+Q_{10})$
Air supply pipelines outlet	$Q_9=Q_8$	$T_9=T_8+\Delta T$
Recycled air pipe	$Q_{10}=Q_1$	$T_{10}=T_{cabin}$

where:
Q = mass flow rate
T = temperature
N = number of passengers in the cabin
q = amount of fresh air required for each passenger (0.0067 kg/s)
π_c = compression ratio of compressor (2.5)
π_t = expansion ratio of turbine (4)
η_{PHE} = efficiency of primary heat exchanger (0.8)
η_{MHE} = efficiency of main heat exchanger (0.85)
η_c = compressor efficiency (0.75)
η_t = turbine efficiency (0.65)
k = specific heat ratio of air (1.4)
ΔT = temperature rise (positive value) or temperature drop (negative value)

Subscript numbers are defined in Figs. 3 and 4.

During flight, the ECS controls the thermal environment of the cabin by means of air temperature. The temperature of set-point in the cabin is based on the thermal comfort requirements of passengers and crew members. The air temperature sensor is assumed to be located 0.03 m below the ceiling in the center of the cabin. The ECS regulates the supply air temperature through the flow valve as shown in Fig. 3 by means of a PID logic controller.

ANSYS Simplorer (ANSYS, 2014a) has multiple computational modules with which this investigation implemented the ECS models through user definitions and which can perform the ECS operations. The built-in PID control module in Simplorer can be easily used to control the temperature.

2.3 CFD model of the cabin environment

ANSYS Fluent, a CFD program, was used in this investigation to transiently model the air environment in a cabin. Our study used an MD-82 cabin as an example. The detailed information about the geometry and boundary conditions can be seen in Duan et al. (2015). Because of our limited computing resources, we did not simulate the entire MD-82 air cabin, but only the first-class cabin as shown in Fig. 5(a). This study used an unstructured tetrahedral mesh with about 6.4 million cells as shown in Fig. 5(b) for the first-class cabin, as did by Duan et al. (2015).

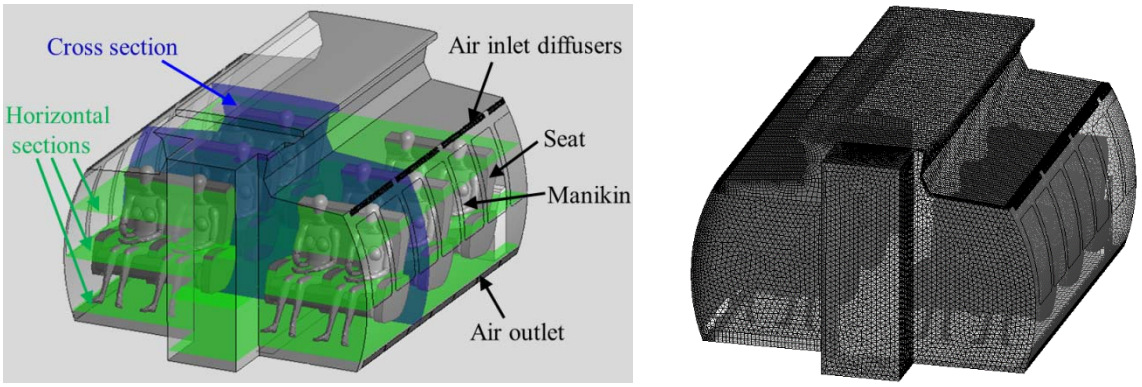

(a) (b)

Fig. 5. The MD-82 first-class cabin studied: (a) cabin geometry with passengers and (b) computational mesh.

The simulations used an unsteady RNG k-ε model and the enhanced wall functions for solid surfaces. The SIMPLE algorithm was used to couple pressure and velocity equations. The PRESTO! scheme was employed for pressure discretization, and the first-order upwind scheme was used for momentum, turbulent kinetic energy, turbulent dissipation rate, and energy. More detailed information can be found in the ANSYS Fluent manual (ANSYS 2014). The inner wall boundary temperature was calculated by the external temperature and heat transfer coefficients of the fuselage in the equations presented in the literature (ASHRAE, 2011). The supply air temperature was obtained from the ECS models. The surface temperature of the manikins was specified as constant

at 302 K. The air outlet pressure on both sides near the cabin floor was assumed to be constant.

During flight, the cabin pressure should not be less than the cabin pressure altitude of 2440 m or 0.74 atm (ASHRAE 2013). In this study, we assumed that the cabin pressure changed gradually with ambient pressure, and that the cabin pressure was 0.74 atm at the maximum cruising altitude of 10 km above sea level. Therefore, the cabin pressure changed according to the pressure schedule described by Eq. (4). Fig. 6 shows the cabin pressure schedule in this study, where pressure changed with flight altitude.

$$p_{schedule} = p_h + \frac{1}{n}(p_{h0} - p_h) \tag{4}$$

where $P_{schedule}$ is the pressure schedule, n the pressurization rate (n = 1.53 in this study), P_h the atmospheric pressure at flight altitude h, and P_{h0} the pressure at sea level.

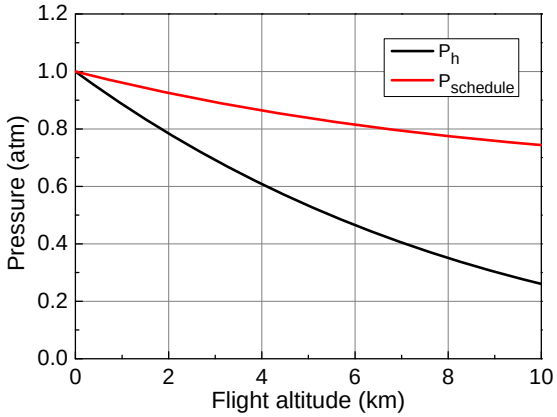

Fig. 6. The cabin pressure schedule used in this study.

To guarantee the mass flow rate of supply air for passengers, the velocity from the air supply diffusers should satisfy the ideal gas equation:

$$v_s = \frac{mRT_s}{P_{schedule}S} \tag{5}$$

where v_s is the air velocity at the supply diffuser outlet; m the mass flow rate, which is Q_9 in Table 1; R the air constant (R = 0.2865 kJ/kg·k); T_s the temperature of the supply air; and S the total area of the air inlet diffuser in the cabin model (S = 0.13133 m^2 in our study).

It should be noted that the computational mesh in Fig. 5(b) was used for in-flight calculations with a fully occupied cabin. To simulate an empty cabin while the aircraft is on the ground before boarding, an unstructured tetrahedral grid with 5.9 million cells was used.

2.4 Coupled simulations

Coupling of the ECS model in ANSYS Simplorer with the cabin environment model in ANSYS Fluent can provide dynamic control of the thermal environment in the cabin. This coupling allows the exchange of data between the two models, which is critical for obtaining accurate results. Fig. 7 is a schematic diagram of the data exchange in the

coupled simulations at time $k\Delta t$. Fig. 7(a) represents ground operation and Fig. 7(b) in-flight operation. The difference between the two was the feedback signal, which was the supply air temperature (T_s^k) on the ground and the cabin air temperature in flight. Let us take the flight process as an example. In Fig. 6(b), T_{set} is the set-point air temperature for the cabin; T^k_f is the actual air temperature in the cabin (0.03 m below the ceiling in the center of the cabin), which can be determined by CFD; and T^k_{dev} is the temperature deviation between T_{set} and T^k_f. The controller used T^k_{dev} to determine Q^k_b, which is the bypass flow rate through the flow valve in ECS or an input for Simplorer. T^k_s is the supply air temperature, which is an output from the ECS or an input to Fluent for the air cabin. The superscript k is the number of time steps in the coupled simulations.

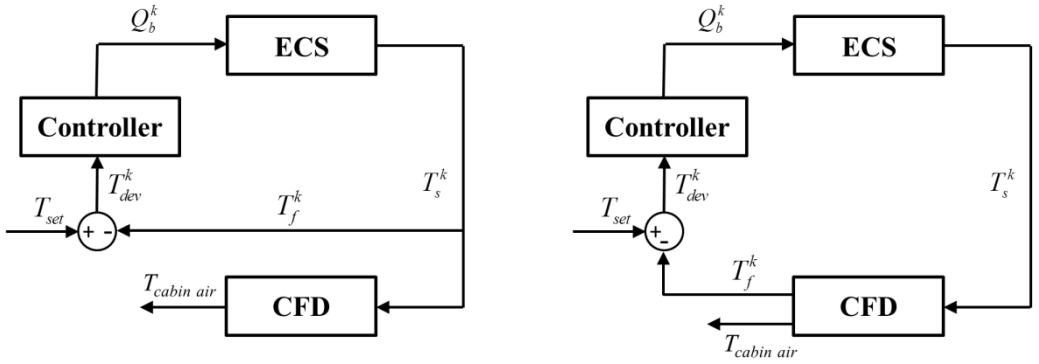

Fig. 7. Schematic diagram of data exchange in the coupled simulation at time $k\Delta t$: (a) on the ground and (b) in flight.

Note that the controller determined Q^k_b on the basis of PID logic by means of the following equation:

$$Q_b^k = \alpha[K_p(T_{dev}^k + \frac{1}{K_i}\sum\nolimits_1^k T_{dev}^j \Delta t + K_d \frac{dT_{dev}^k}{\Delta t})] \quad (6)$$

where α is a conversion coefficient from T_{dev} to Q_b; K_p, K_i, and K_d are the proportional, integral, and differential terms, respectively, used in control logic; and Δt is the time step size.

2.5 Experimental measurements for validating the coupled model

This investigation used a retired MD-82 commercial airplane to obtain experimental data for validating the coupled model of the ECS and air cabin environment for ground operation. Fig. 8(a) shows the MD-82 experimental platform at Tianjin University used in this study. A GAC supplied conditioned air to the airplane cabin for regulating the cabin's thermal environment.

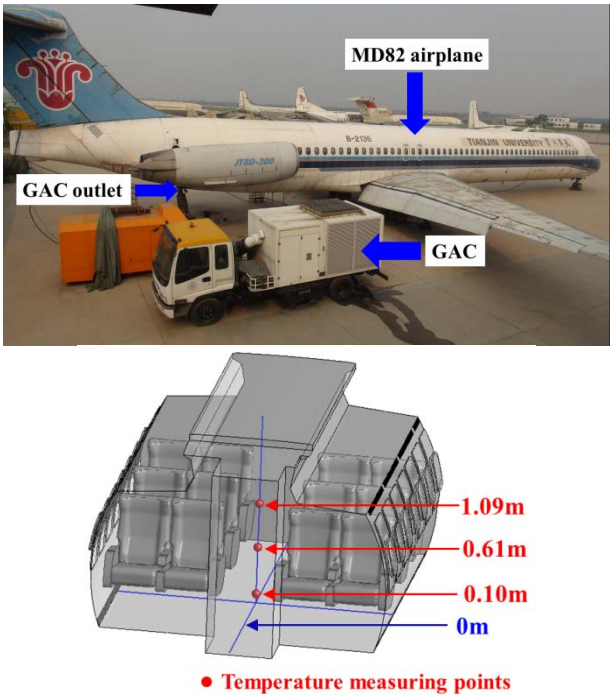

Fig. 8. (a) The MD-82 airplane with a GAC and (b) the measuring points for air temperature in the cabin.

The experiment was conducted on the ground on a winter morning when the outside air temperature was below 0 ºC; the air temperature in the cabin was also below 0 ºC after the airplane had been parked overnight. The cabin was heated to approximately 20 ºC to provide a suitable thermal condition. During the experiment, the cabin doors were closed and 1.35 m^3/s (9.2 L/s per passenger) of heated air was supplied to the cabin by the GAC. The maximum heating power of the GAC was 79 kW, and the heating capacity was regulated by the temperature controller base on the PID logic with K_p = 27.6, K_i = 240, and K_d = 21. The temperature sensor at the GAC outlet was used for controlling the temperature of air supply in GAC outlet, and the set-point temperature of the air supply was 40 ºC.

This investigation continuously measured the air temperature at the GAC outlet and cabin diffuser outlets for validating the ECS model in Simplorer. Meanwhile, the air temperatures in the cabin were measured at different positions, as shown in Fig 8(b), for validating the cabin model in Fluent. These positions were at heights of 0.10 m, 0.61 m, and 1.09 m above the floor, which represent the ankle, waist, and head levels, respectively, of seated passengers (ASHRAE 2013). The cabin air temperatures would also be used for evaluating the thermal environment in the cabin. The experiment used T-type thermocouples to measure the temperatures. The thermocouples had a precision of ±0.5 K, and the sampling frequency was 1 Hz.

3 Results

This section first compares the GAC and cabin air temperatures for ground operation obtained by the coupled model with the measured data. Next, the use of the coupled model to simulate the interaction between ECS operation and cabin thermal environment

for in-flight operation is discussed. Finally, this section presents an analysis of the impact of ECS operation control on the cabin thermal environment.

3.1 Validation of the coupled simulation for ground operation

Fig. 9 compares the calculated air temperatures at the GAC outlet and the cabin air diffuser outlets with the measured temperatures. The calculated results are in good agreement with the experimental data. A small discrepancy was found at the GAC outlet between 10 and 20 minutes after the GAC was turned on. The reason for this discrepancy was that the actuation time via PID controller for the actuators in the GAC system was different for the experiment than for the simulation model. Therefore, the temperature calculated by the model was higher than the measured temperature, and the set-point temperature was reached faster in the calculations. Since this small discrepancy should be acceptable, the ECS model implemented in ANSYS Simplorer for ground conditions performed as expected.

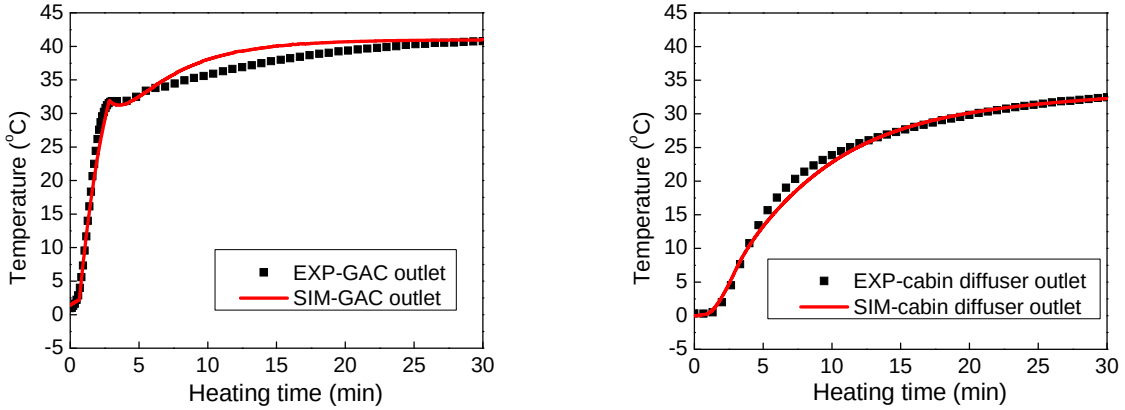

Fig. 9. Comparison of the calculated GAC and cabin air temperatures with measured temperatures during ground operation: (a) at the GAC outlet and (b) at the cabin diffuser outlets.

Fig. 10 compares the air temperatures in the cabin calculated by ANSYS Fluent with the experimental data at the three positions shown in Fig. 8(b). The simulated air temperatures agree well with the experimental data. The results show vertical temperature stratification throughout the heating process. After 30 minutes, the air temperature at head level reached 18.3 °C, which was sufficient for boarding (ASHRAE 2013). Although the air temperature below head level was still low, passengers' movements during boarding would enhance the mixing of air. The aircraft requires more than 30 minutes to heat up its cabin as obviously seen in Figure 10. However, in this validation experiment, the measurements were conducted for only 30 minutes because the external air temperature and solar radiation conditions changed rapidly and unpredictably in the winter morning. We were not allowed to take early measurements due to noise control on the campus in the morning. When the winter clothing level is taken into account, the thermal environment is capable of providing acceptable thermal comfort for passengers and crew.

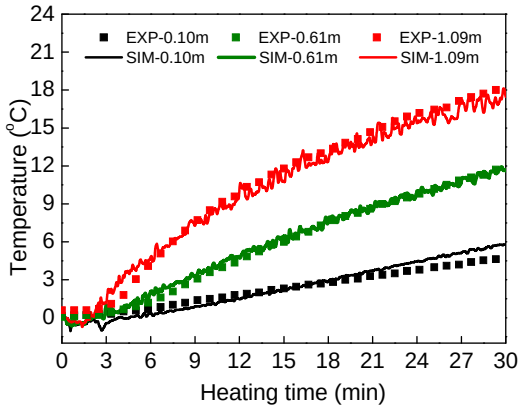

Fig. 10. Comparison of calculated air temperatures with experimental data in the cabin at heights of 0.10 m, 0.61 m, and 1.09 m above the floor.

3.2 Coupling Simplorer and Fluent Simulation for In-flight Operation

The comparison of the air temperatures calculated by Simplorer and Fluent with the corresponding experimental data confirmed the reliability of the model developed in this study. This investigation further applied the model to a short flight of 3340 s to simulate the interaction between the ECS and the cabin thermal environment. The flight consisted of 4 minutes for taxiing from the terminal to the runway, 1 minute for takeoff from the runway, 15 minutes for climbing to the cruising altitude of 10 km, 5 minutes for cruising, 20 minutes for descending, 40 seconds for landing, and 5 minutes for taxiing to the terminal. Fig. 11 shows the flight altitude and cabin pressure schedule at different stages of the flight. The rapid changes in ambient temperature and pressure during the flight would have influenced the thermodynamic processes of the ECS and the boundary conditions of the cabin. The ambient air temperature was assumed to be 0 ºC on the ground and then changed at a rate of -6.5 ºC/km altitude. The cabin air temperature was initiated at 23 ºC. Meanwhile, the cabin air temperature should be maintained at 23 ºC during the entire flight process (ASHRAE 2013) thereby the set temperature in PID controller was 23 ºC as well.

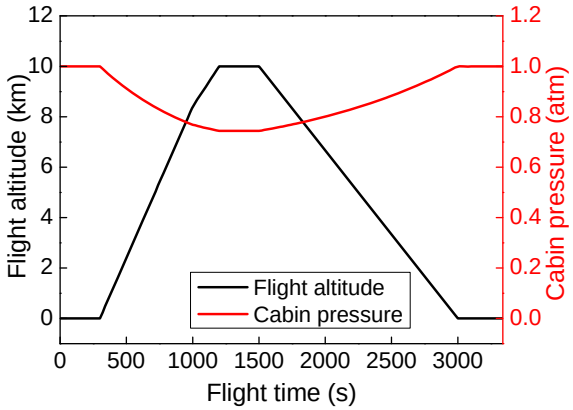

Fig. 11. The aircraft altitude and cabin pressure during the flight.

Throughout the entire flight process, the aircraft ECS was regulated to maintain a stable thermal environment in the cabin. Fig. 12(a) compares the cabin air temperature at the feedback point during the flight with the set-point temperature. The temperature at the

feedback point was lower than the set-point value during the climbing process and higher than the set-point value during the descending process. This difference is due to the fact that the ambient temperature decreased gradually during the climbing process and increased gradually descent. However, with the PID controller the temperature at the feedback point was stable within a range during the entire flight. The temperature difference between the feedback point and set point was smaller than ±0.6 K, which was within the ±1.1 K required by the ASHRAE standard (ASHRAE 2013).

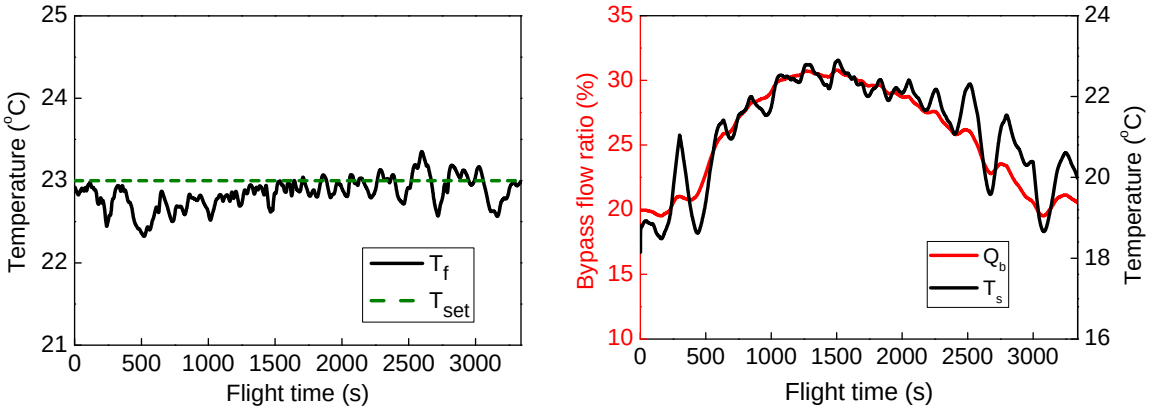

Fig. 12. (a) The controlled cabin air temperature and (b) the bypass flow ratio of the bleed air in the ECS and the temperature of the supply air to the cabin.

Fig 12 (b) shows the bypass flow ratio of the total bleed air in the ECS and the temperature of the supply air to the cabin during the entire flight process. As shown in Fig. 3, the bypass flow ratio was controlled directly by the PID controller through the flow valve. At the beginning of the process, the cabin air temperature changed slightly, and thus the bypass flow ratio had a small change as well. The bypass flow ratio then increased during the climbing stage because of the increasing thermal load in the cabin, and the reverse trend can be observed in the descending stage. The maximum bypass flow ratio was reached in the cruising stage because the thermal load in the cabin was the highest while the outside air temperature was the lowest. The supply air temperature increased with the increase in bypass flow ratio, and thus the highest supply air temperature was likewise found in the cruising stage. However, the supply air temperature fluctuated to a greater extent than the bypass flow ratio because the supply air temperature was also influenced by the air temperature at the turbine outlet and the return air temperature, which would have changed with the flight stage and time. The mean supply air temperature in the cruising state was about 22.5 °C, which is lower than the cabin air temperature of 23 °C, because more heat was released by the 12 manikins than was loss through the walls. The air temperatures and bypass flow ratio simulated by Simplorer indicate excellent control.

Figs. 13 and 14 show the air temperature distributions in the cabin as calculated by Fluent. Fig. 13 depicts the distributions in a cross section (see Fig. 5(a)) at the taxiing, climbing, cruising, and descending stages. The distributions were relatively uniform at the climbing, cruising, and descending stages, when the flow was relatively stable and mixing was good. Fig. 14 shows the temperature distributions at cruising altitude (t = 1346 s) at heights of 0.10 m, 0.61 m, and 1.09 m above the floor (see Fig. 5(a)), which represent the ankle, waist, and head levels, respectively. Because of mixing ventilation,

the temperatures at the three heights were nearly the same, except in close proximity to the manikins where thermal plumes played a role. Therefore, the thermal environment in the cabin was acceptable for passengers and crew according to the ASHRAE standard (ASHRAE 2013).

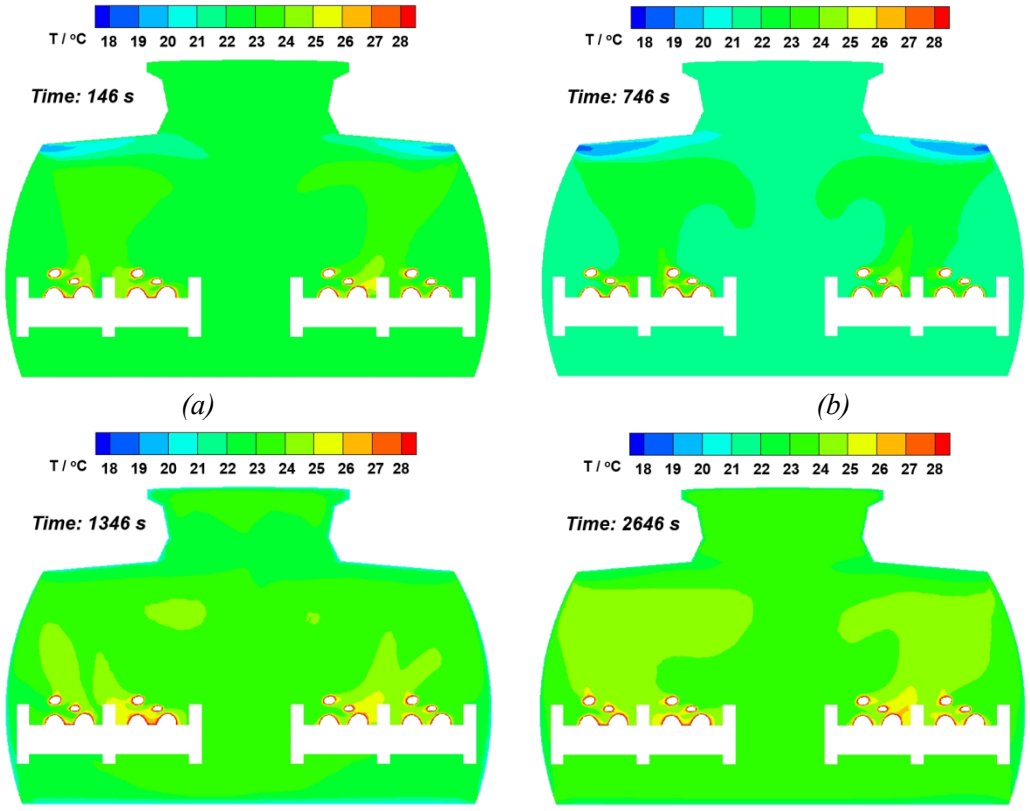

Fig. 13. The air temperature distributions in a cross section (see Fig. 5(a)) of the cabin at different stages of the flight: (a) taxiing, (b) climbing, (c) cruising, and (d) descending.

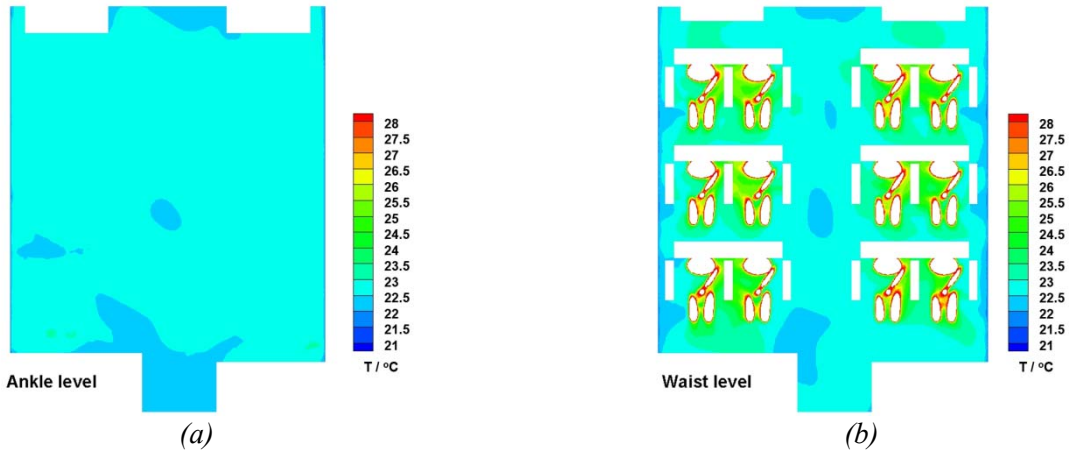

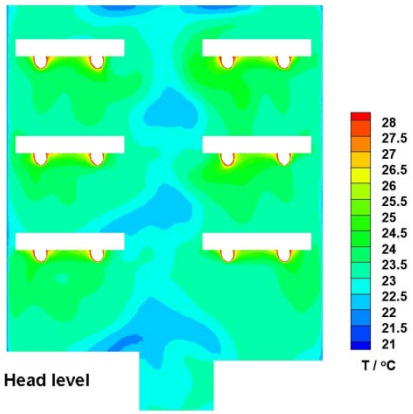

(c)

Fig. 14. The air temperature distributions at (a) 0.10 m (ankle level), (b) 0.61 m (waist level), and (c) 1.09 m (head level) above the cabin floor (see Fig. 5(a)) when the airplane was in the cruising stage (t = 1346 s).

4 Discussion

Simplorer is a one-dimensional model that requires little computing effort. In contrast, CFD simulations by Fluent solve three-dimensional, partial differential equations that are very time consuming. In this study, more than 99% of the time required for the coupled simulations was used by Fluent. For example, in the coupled simulation of a 3340 s flight with a time step size of 0.3 s, only a few seconds of computing time were consumed by Simplorer, while about 60 hours were used by Fluent. Although CFD can provide very detailed information, this level of detail is not necessary for control purposes. A reduced-order model (Kim et al. 2015) would reduce the computing effort required by CFD and would thus be more appropriate.

In the experiment, the GAC controlled the supply air temperature with a time step of 5.0 s. In our simulation, as shown in Fig. 9, the time step was 0.3 s. The smaller step size was used to ensure that the PID controller provided better control in the numerical simulations. Fig. 15 compares the air temperatures at the GAC outlet, the cabin diffusers, and the three heights in the cabin with time steps of 0.3 s and 1.0 s for the purpose of control. The temperature profiles with the two time step sizes are almost identical. Thus, it is not necessary to use very small time steps in the coupled simulations. Moreover, the computing time with the time step of 0.3 s was about two times longer than that with the 1.0 s time step. Since the time step size is crucial for reducing the computing cost, a large time step should be used if possible.

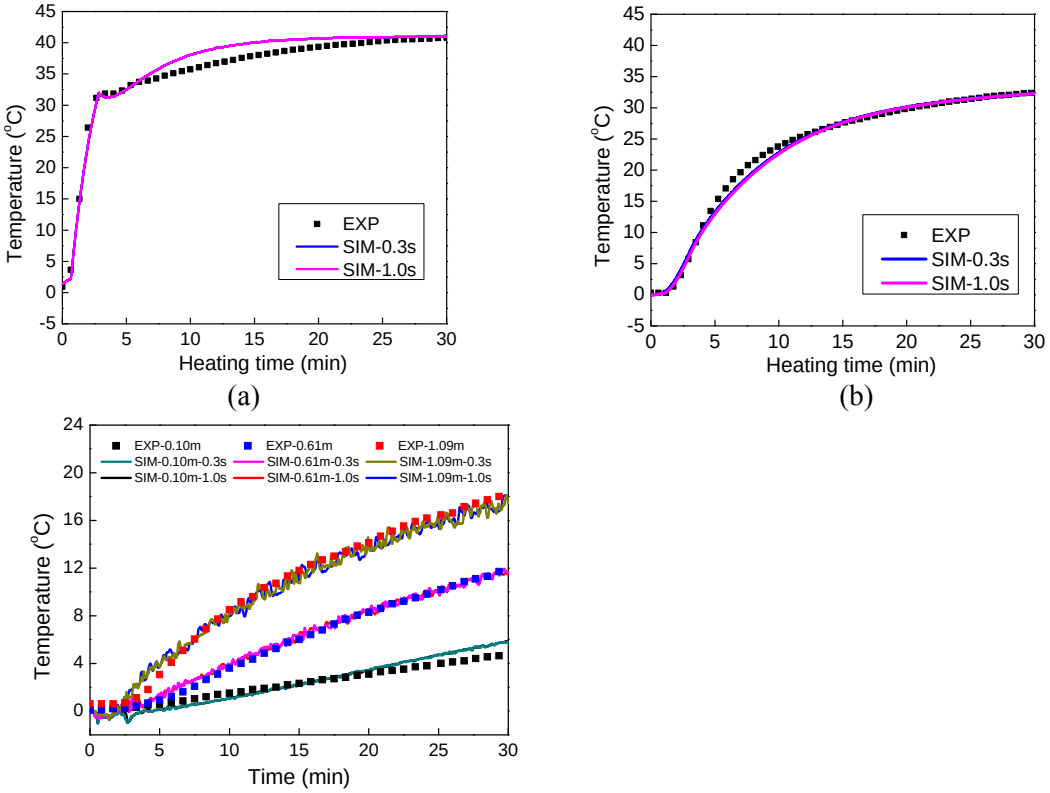

Fig. 15. The effects of time step size in the coupled model on the air temperature (a) at the GAC outlet, (b) at the cabin diffusers, and (c) at different heights in the cabin.

5 Conclusions

This investigation developed a model for ECS operation on the ground and in flight in ANSYS Simplorer. The thermal environment in an airplane cabin was simulated by ANSYS Fluent. Coupling of Simplorer and Fluent makes it possible to simulate transient control of the ECS and the cabin environment. The simulated air temperatures at various locations were compared with the experimental data obtained in an MD-82 aircraft cabin on ground. The study led to the following conclusions:

The simulated air temperatures at the outlets of the GAC and cabin air diffusers agree with the measured data obtained from an MD-82 airplane and a GAC in ground operation. This comparison implied that the coupled simulations were reliable for simulating the interaction between the indoor thermal environment and the ECS.

Coupled simulations were also conducted for in-flight operation. The results show that the PID controller used in the ECS can effectively maintain the cabin air temperature at a level that provides acceptable thermal comfort for passengers and crew members.

The CFD simulations of thermal environment by Fluent were very time consuming. To reduce computing costs, the time step size used in the simulations could be increased without compromising accuracy.

Nevertheless, this study provided useful information for numerically testing the performance of ECS and evaluating the thermal environment in a cabin during aircraft design.

References

ANSYS (2014). ANSYS Fluent Version 15.0. ANSYS, Inc.

ANSYS (2014a). ANSYS Simplorer Version 15.0. ANSYS, Inc.

ASHRAE Handbook- HVAC Application (2011). American Society of Heating, Refrigerating and Air-Conditioning Engineers, Inc. (www.ashrae.org).

ASHRAE (2013). Air Quality within Commercial Aircraft. In: ANSI/ASHRAE Standard 161-2013. Atlanta, USA: ASHRAE.

Chen C, Lin C.H, Long Z, Chen Q (2014). Predicting transient particle transport in enclosed environments with the combined CFD and Markov chain method. *Indoor Air,* 24: 81-92.

Duan R, Liu W, Xu L, Huang Y, Shen X, Lin C.H, Liu J, Chen Q, Sasanapuri B (2015). Mesh type and number for CFD simulations of air distribution in an aircraft cabin. *Numerical Heat Transfer,* Part B: Fundamentals, 67(6): 489-506.

Eichler J (1975). Simulation study of an aircraft's environmental control system dynamic response. *Journal of Aircraft,* 12(10): 757-758.

Hofman J.M.A (2003). Control–fluid interaction in air-conditioned aircraft cabins: A demonstration of stability analysis for partitioned dynamical systems. *Computer Methods in Applied Mechanics and Engineering,* 192(44): 4947-4963.

Huang Y, Li J, Li B, Duan R, Lin C.H, Liu J, Shen X, Chen Q (2015). A method to optimize sampling locations for measuring indoor air distributions. *Atmospheric Environment,* 102: 355-365.

Hu X, You X (2015). Determination of the optimal control parameter range of air supply in an aircraft cabin. *Building Simulation,* 8(4): 465-476.

Kim D, Braun J.E, Cliff E.M, Borggaard J.T (2015). Development, validation and application of a coupled reduced-order CFD model for building control applications. *Building and Environment,* 93(2): 97-111.

Leo T.J, Pérez-Grande I (2005). A thermoeconomic analysis of a commercial aircraft environmental control system. *Applied Thermal Engineering,* 25: 309-25.

Li M, Zhao B, Tu J, Yan Y (2015). Study on the carbon dioxide lockup phenomenon in aircraft cabin by computational fluid dynamics. *Building Simulation,* 8(4): 431-441.

Liu W, Chen Q (2015). Optimal air distribution design in enclosed spaces using an adjoint method. *Inverse Problems in Science and Engineering,* 23(5): 760-779.

Liu W, Mazumdar S, Zhang Z, Poussou S.B, Liu J, Lin C. H, Chen Q (2012b). State-of-the-art methods for studying air distributions in commercial airliner cabins. *Building and Environment,* 47: 5-12.

Liu W, Wen J, Chao J, Yin W, Shen C, Lai D, Lin C.H, Liu J, Sun H, Chen Q (2012a). Accurate and high-resolution boundary conditions and flow fields in the first-class cabin of an MD-82 commercial airliner. *Atmospheric Environment,* 56: 33-44.

Mazumdar S, Long Z, Chen Q (2014). A coupled CFD and analytical model to simulate airborne contaminant transmission in cabins. *Indoor and Built Environment,* 23: 946-954.

Ordonez J.C, Bejan A (2003). Minimum power requirement for environmental control of aircraft. *Energy,* 28: 1183-202.

512 Pérez-Grande I, Leo T.J (2002). Optimization of a commercial aircraft environmental
513 control system. *Applied thermal engineering,* 22(17): 1885-1904.
514 Poussou S, Mazumdar S, Plesniak M.W, Sojka P, Chen Q (2010). Flow and contaminant
515 transport in an airliner cabin induced by a moving body: Scale model experiments
516 and CFD predictions. *Atmospheric Environment,* 44(24): 2830-2839.
517 World Bank Group (Ed.) (2015). 2015 World Development Indicators. World Bank
518 Publications.
519 Zhang Z, Chen X, Mazumdar S, Zhang T, Chen Q (2009). Experimental and numerical
520 investigation of airflow and contaminant transport in an airliner cabin mockup.
521 *Building and Environment,* 44(1): 85-94.
522 Zhao H, Hou Y, Zhu Y, Chen L, Chen S (2009). Experimental study on the performance
523 of an aircraft environmental control system. *Applied Thermal Engineering,* 29(16):
524 3284-3288.